

# An experimental comparison of PID autotuners<sup>☆</sup>

Josefin Berner<sup>\*</sup>, Kristian Soltesz, Tore Hägglund, Karl Johan Åström

Department of Automatic Control, Lund University, Sweden

## ARTICLE INFO

### Keywords:

PID control  
Automatic tuning  
Process industry  
Relay feedback  
Comparative study

## ABSTRACT

In this paper two novel autotuners are compared with two industrially available ones. The aim is to see if the research frontline can improve the industry standard of today. Experiments are made on three laboratory processes with different characteristics. Two lag-dominated processes of which one is a level control problem with fast dynamics, and one a temperature control problem with slow dynamics, as well as one delay-dominated level control process. Both the experiments and the obtained controller performances are evaluated and discussed. The results show that the performance of the state-of-the-art industrial autotuners can be significantly improved.

© 2018 Published by Elsevier Ltd.

## 1. Introduction

Automatic tuning of PID controllers is a useful feature for any user who does not have the time, knowledge or desire to manually tune his or her control loops. Especially in the process industry, where a factory may have hundreds or thousands of different flows, levels, temperatures, concentrations etc. that need to be controlled, the benefit of a fast and reliable way of finding appropriate controller parameters is large. One such procedure that is common in industry is the relay autotuner.

The principle of relay autotuning is as follows. By closing the feedback loop with a relay function, that switches between two values depending on the process output, the process is forced into oscillations. See Fig. 1 for the setup and Fig. 2 for a typical experiment output. From the oscillations process data can be obtained and used to tune a PID controller. The original relay autotuner (Åström & Hägglund, 1984) uses the period time and amplitude of the induced oscillations in order to find the critical point where the process Nyquist plot intersects the negative real axis. If a hysteresis band is added to reduce shattering due to noise, a slightly different point is obtained. The controller parameters are then found by moving this point to give the open-loop system specified amplitude and phase margins.

The autotuner from Åström and Hägglund (1984), that was developed in the 1980's, is probably still the most common one in industrial DCS systems today. Several of the major vendors use this procedure. It has been implemented in industrial control systems such as the ABB ECA600, the ABB 800 XA and it is also the base of the autotuner feature in e.g. Emerson Delta V. Even though the knowledge about PID control has been improved and the available computing power of

control systems has increased dramatically since the 1980's, it does not seem to have affected available industrial autotuners much. In academic literature many modifications and improvements have been suggested to the relay autotuner. For instance Friman and Waller (1997), Li, Eskinat, and Luyben (1991) and Luyben (1987), have modified the autotuner to find first- or second-order models with time delay of the process instead of a single frequency point. The excitation of the process has also been improved by the usage of asymmetric relay functions in e.g. Kaya and Atherton (2001) and Shen, Wu, and Yu (1996). A review of the current state of process modeling from relay experiments can be found in Liu, Wang, and Huang (2013). However, these improvements do not seem to have made their way out to the industrial products.

The question we aim to answer in this paper is whether this is since the old autotuners are performing well-enough, or if they could actually be significantly improved by including recent scientific development. In order to do that, we compare two new autotuners developed by the authors, to the ABB ECA600 (ABB, 1999) containing the traditional autotuner (Åström & Hägglund, 1984) and the more recent autotuning algorithm Accutune III™ provided in the Honeywell UDC3200 (Honeywell, 2012). Since the autotuners are mainly used in industrial settings, a simulation study would not cover typical problems. Consequently the comparisons will be performed on laboratory processes that feature many of the issues encountered in practice like noise, non-linearities, disturbances, low converter resolutions etc.

Even if the autotuning possibility has been available in most control systems for some decades it is not always used, resulting in unnecessarily poor control performances in many systems (Desborough & Miller, 2002;

<sup>☆</sup> The authors are members of the LCCC Linnaeus Center and the ELLIIT Excellence Center at Lund University.

<sup>\*</sup> Corresponding author.

E-mail address: [josefin.berner@control.lth.se](mailto:josefin.berner@control.lth.se) (J. Berner).

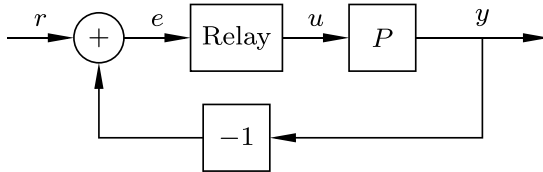


Fig. 1. Setup for the relay feedback experiment, where  $r$  is the constant reference value,  $e$  is the control error,  $u$  is the relay output and  $y$  is the process output.

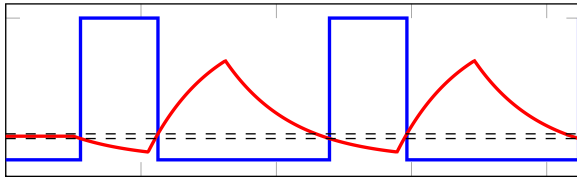


Fig. 2. Outputs from a relay feedback experiment. The relay output  $u$  (blue) switches between its two values every time the process output  $y$  (red) leaves the hysteresis band (dashed black), causing the process to oscillate. If the amplitudes of the relay function are different, as in this figure, the relay is said to be asymmetric. (For interpretation of the references to color in this figure legend, the reader is referred to the web version of this article.)

Ender, 1993; Kano & Ogawa, 2010). Reasons for this may be that the users are either not aware of the feature or do not feel confident in using it. Therefore it is important to ensure that the autotuners, apart from giving satisfactory results, are easy to understand and use also for non-experienced users. In this study we will therefore do as few manual interactions as possible with the autotuner settings, and will not assume any knowledge of neither the process nor control theory.

## 2. The study

This study compares and evaluates four different autotuners, described in Section 3, on three processes that are described in Section 4. The autotuners are evaluated on their experiment durations, their user-friendliness, and on the performance of the obtained controllers. Since the industrial autotuners do not provide the user with any models that they base the controller designs on, no comparison can be made between estimated models.

Three experiments are run by each autotuner, and a representative controller setting is chosen for comparison to the other autotuners. The multiple experiments are performed in order to reduce the risk of disturbances affecting the result of one of the autotuners causing an unfair comparison. All obtained controller parameters are presented in Section 5, along with the performance experiments.

The most important aim for a controller in process industry is to be able to handle load disturbances, and the performance tests in this comparison are therefore focused on load disturbance attenuation. The disturbances were designed and controlled to ensure that identical disturbances affected each of the controllers on the specified process.

## 3. The autotuners

The four autotuners used in this study are presented in this section. As stated in the introduction the aim is to compare industrial standard autotuners to recent developments in academic literature. The selection of industrial autotuners include the ABB ECA600 further described in Section 3.1 and the Honeywell UDC3200 described in Section 3.2. A motivation to this choice is that we wanted one autotuner containing an implementation of the original procedure from Åström and Hägglund (1984), which is still the most common one, as well as one more recent version of a relay autotuner available on the market today. By this choice we want to find out what improvements have been made in

the industrial controllers during the last 30 years. There are of course other brands and procedures that could have been chosen, as well as completely different autotuning principles based on step responses or other open-loop experiments. We did, however, restrict this study to only contain relay autotuners.

The academic autotuners we selected are implementations of two versions developed by the authors. The  $\tau$ -tuner, described further in Section 3.3, is procedure-wise very similar to the original autotuner, but has some modifications to obtain better models. The NOMAD autotuner, described in Section 3.4, utilizes more data and requires more computational power, but allows for shorter experiment times. We could have chosen to include many other academic autotuners in this study, e.g. the ones presented in Chidambaram and Sathe (2014), Keyser, Joita, and Ionescu (2012) and Yu (2006). Since we did not have any implementations of these autotuners, and since we wanted to find out how our proposed autotuners compared to the industry standard, we decided to restrict ourselves to this selection.

### 3.1. ABB ECA600

The ABB ECA600 controller, in this paper referred to as ECA, is shown in Fig. 3. The operator's manual (ABB, 1999) describes it as “... a dual loop controller with advanced control functions. In addition the ECA600 has comprehensive logical and arithmetical data processing facilities. Its five analog inputs, three analog outputs, four digital inputs and six digital outputs can be used to solve almost any process control problem”.

The built-in autotuner is based on (Åström & Hägglund, 1984) and provides PID parameters for a controller on serial form immediately from the experiment. The autotuner is accessible after enabling it in the configuration menu. Before starting the tuning the user has to make sure that the process value is in steady state close to the setpoint, otherwise the tuning may fail. The autotuner starts by measuring the noise level for 5 s to set an appropriate hysteresis level. The relay amplitudes are restricted to 10% of the control interval by default. If the autotuner notices that the process variable deviations are too large (or too small) during the experiment it will adjust the relay amplitudes if the restrictions allow it. The PID controller includes a first-order filter for the derivative part of the controller with a filter time constant  $T_f = T_d/8$ .

There is an option to tell the autotuner whether the controller dynamics should be Normal, DeadTime, PI or pPI. Since this study focuses on how an unexperienced user would be able to use the autotuners, we do not assume to have this kind of knowledge and hence always use the default Normal.

### 3.2. Honeywell UDC3200

To compare with a more recent controller we chose the Honeywell UDC3200 with the autotuning feature Accutune III™. The Honeywell UDC3200, in this paper referred to as Honeywell, is shown in Fig. 4. According to its manual (Honeywell, 2012) it is “... an ideal controller for regulating temperature and other process variables in numerous heating and cooling applications, as well as in metal working, food, pharmaceuticals, semiconductor, testing and environmental work”. In spite of being mainly considered as a temperature controller, the manual (Honeywell, 2012) also claims that “This standard feature [read: Accutune III™] provides a truly plug and play tuning algorithm, which will, at the touch of a button or through a digital input, accurately identify and tune any process including those with deadtime and integrating processes”.

The tuning can be started whenever TUNE has been enabled in the setup menu, but to start the autotuner the controller must be switched to automatic mode. A choice between SLOW and FAST tuning can be made. This does not affect the experiment, but calculates the controller parameters differently. Since we do not assume to know anything about the process we used the SLOW option for all experiments. The autotuner switches the relay output two full cycles between the maximum and minimum control output levels, independent of the setpoint value.



Fig. 3. The ABB ECA600 controller.

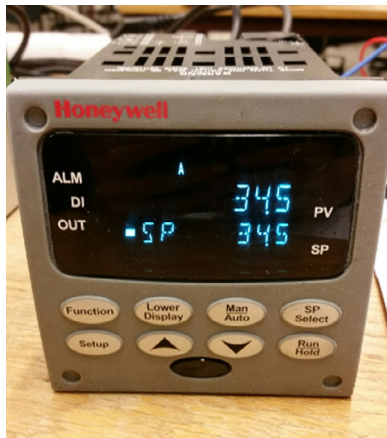


Fig. 4. The Honeywell UDC3200 controller.

PID parameters for a controller on serial form are obtained from the experiment and immediately used. As far as we know, this autotuner does not design any filter for the controller, and the only filter used in our experiments is a noise filter with the default time constant value 1 s.

### 3.3. $\tau$ -tuner

The autotuner described in Berner, Hägglund, and Åström (2016a, b) is here denoted as the  $\tau$ -tuner. It uses an asymmetric relay function with adjustable amplitudes and runs until limit cycle convergence is reached. From the relay oscillations it uses the half-period times and the integral of the process output over one cycle, to calculate an integrating or first-order model with time delay of the process. It then uses the AMIGO (Åström & Hägglund, 2006) tuning rules to obtain parameters for a PI or PID controller on parallel form. It uses the normalized time delay,  $\tau$ , to select model and controller structure. The normalized time delay is defined as

$$\tau = \frac{L}{L + T}, \quad (1)$$

where  $L$  is the deadtime and  $T$  is the time constant of the process dynamics. More details about how the autotuner utilizes  $\tau$  can be found in Berner et al. (2016b). The  $\tau$ -tuner is simple to implement and use,

but as was stated in Berner et al. (2016a) it can be quite sensitive to quantization, non-linearities and non-stationary starting conditions. The autotuner setup in these experiments uses a restriction on the large relay amplitude to be maximum 10% of the available control range, it uses 10 s in the beginning of the experiment to measure noise and decide on a hysteresis level, but also has a minimum hysteresis level of 0.5% of the process output range.

In the papers (Berner et al., 2016a, b), no filter was designed for the controller. Since we need some roll-off for high frequencies to reduce the impact of noise, we let the autotuner design a second order filter on the form

$$F(s) = \frac{1}{1 + sT_f + (sT_f)^2/2}. \quad (2)$$

The filter time constant  $T_f$  is chosen as

$$T_f = \frac{1}{5\omega_{180}}, \quad (3)$$

where  $\omega_{180}$  is the frequency where the estimated process model has a phase lag of 180°. The filter  $F(s)$  is used on the entire controller, not only the derivative part.

The model, filter, controller parameters and some additional experiment data are available to the user of this autotuner.

### 3.4. NOMAD-autotuner

The experiment and modeling part of the *Noise-robust Optimization-based Modeling And Design Autotuner* (NOMAD) is described in Berner and Soltesz (2017). This autotuner performs the same experiment as the  $\tau$ -tuner, with two exceptions. The first exception is that it does not have to be initiated in steady-state, since it estimates the initial conditions. The second exception is that it does not wait for convergence of the limit cycle oscillations but instead stops the experiment after three relay switches. It then uses a gradient-descent algorithm to find first-order or second-order time-delayed models from the entire data set. It chooses which model to use by the Akaike Information Criteria (Akaike, 1974). The usage of the entire data set distinguishes the NOMAD-autotuner from the ECA and  $\tau$ -tuner, that only use certain time intervals, amplitudes etc. to get their models. It can be argued that the need of less data is a benefit of these other methods, but it is also what causes their need to wait for limit-cycle convergence as well as making them more sensitive to noise.

No controller tuning method was specified for the method in Berner and Soltesz (2017) so for this paper we added that to get a complete autotuner. The filter design was chosen the same way as for the  $\tau$ -tuner, hence described by (2) and (3). The controller tuning chosen is the convex-concave optimization method described in Hast, Åström, Bernhardsson, and Boyd (2013). Here the integrated error

$$IE = \int_0^\infty e(t)dt \quad (4)$$

from a step load disturbance on the process input, is minimized with constraints on the maximum values of the sensitivity function

$$S(s) = \frac{1}{1 + P(s)C(s)}, \quad (5)$$

and complementary sensitivity function

$$T(s) = \frac{P(s)C(s)}{1 + P(s)C(s)}. \quad (6)$$

The process  $P(s)$  that is entered to the optimization program is the filtered process, since the controller design and the filter design are connected. The PID parameters obtained are for a controller on parallel form.

Since both the modeling and controller design are optimization-based, this autotuner requires a lot more computations than the original autotuner. However, the calculations performed are rather cheap, and with an efficient implementation and the computing power available today they can be made in the order of seconds.

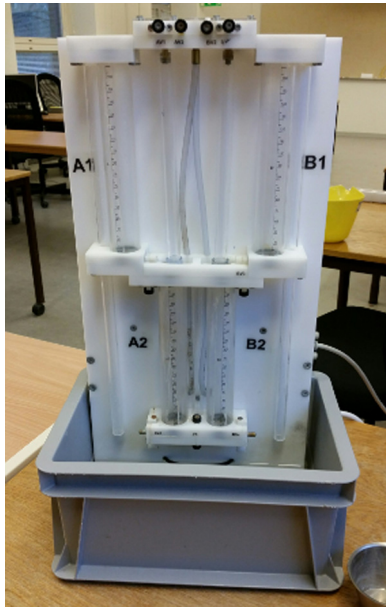


Fig. 5. The quadruple tank used for level control experiments on the lower tank and the delayed upper tank.

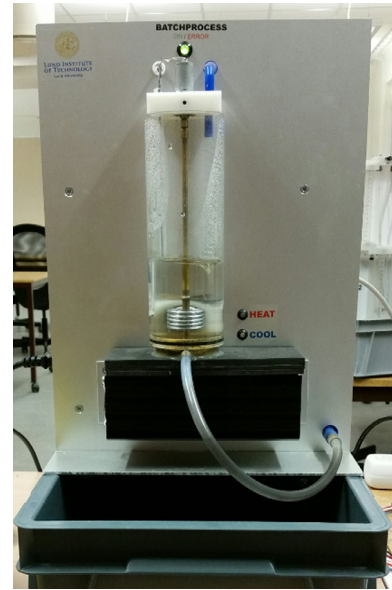


Fig. 6. The batch tank used for temperature experiments.

#### 4. Processes

To evaluate the autotuners on different types of dynamics we chose three processes with different characteristics. Two lag-dominated processes, where one has fast dynamics and one is slow, as well as one process that is delay-dominated. This information about the process dynamics was only used to choose suitable processes and was assumed to be unknown throughout the tuning experiments. The process hardware consisted of a quadruple tank and a batch tank available at the control laboratory at Lund University. Even though the chosen processes are simple, they have significant nonlinearities and noise, making them representative for the processes you encounter in industry. The input and output signals of the processes were normalized to  $u \in [0, 100]$  and  $y \in [0, 100]$ . The processes will be described further in their respective subsections.

##### 4.1. The quadruple tank

The quadruple tank shown in Fig. 5 is a version of the one described in Johansson (2000). The tank can be used as both a single-input single-output system and as a multivariable system. For the experiments in this paper only one side of the quadruple tank was used, in order to get the single-input single-output configuration. This system consists of a pump that pumps water into the upper tank, which then flows through down to the lower tank. For the first experiment, called *Level control*, the measured process variable is the water level of the lower tank. The dynamics can be described by a second-order lag-dominant system with time constants  $T_1$  and  $T_2$ , and an average residence time  $T_{ar} = T_1 + T_2 \approx 20$  s.

The quadruple tank was also used for the delay-dominant process. For the *Delayed tank* experiment, the measured variable was the water level of the upper tank. The dynamics of this process can be described by a first-order system with a time constant  $T \approx 10$  s. To get it delay-dominated a time delay of 20 s was added to the control signal.

##### 4.2. The batch tank

The batch tank is shown in Fig. 6. It consists of one inflow pump, one outflow pump, a heater, a cooler, and an agitator. Measurements

of the water level and temperature are available. For the experiment on this process, referred to as *Temperature control*, we used a fix water level, with both pumps turned off. The agitator was on all the time and a split-range controller was used to control the heater and cooler. The control range of 0–100 was split up so that  $u = 0 - 50$  corresponded to Cooler = 100% – 0% and  $u = 50 - 100$  corresponded to Heater = 0% – 30%. The restriction on the heater was made to balance the heating and cooling capacities of the process.

#### 5. Experiments and results

The results from the three processes are illustrated by plots of the relay experiments as well as the obtained controller performance for load disturbances acting on the process inputs. The choice of performance evaluation was made since decreasing the influence of load disturbances is the main focus in process control (Shinskey, 2002). Before the experiments were started the processes were brought to steady-state at the desired setpoint levels. This startup phase has been discarded in order to only show the actual experiments.

For each process three experiments were made with each autotuner to see how consistent they were. Obtained PID controller parameters for the different experiments are listed in Tables 1–3. Since both the parametrization and the filter design differ between the controllers, a comparison of the Bode plots of the resulting (filtered) controllers are shown for each process. From these results a representative set of parameters was chosen and used for the controller performance experiments. The performance experiments are shown, and the integrated absolute error

$$IAE = \int_0^{t_{end}} |y(t) - r(t)| dt, \quad (7)$$

for each performance experiment, where  $t_{end}$  is the experiment duration, is listed along with the controller parameters in the respective table.

##### 5.1. Level control of the lower tank

A representative relay experiment for each of the autotuners is shown in Fig. 8. Note the differences in experiment duration and signal deviations. This is a rather fast process, hence the short experiment durations. The resulting controller parameters are listed in Table 1 and Bode plots of the (filtered) controllers are shown in Fig. 7. It can be seen



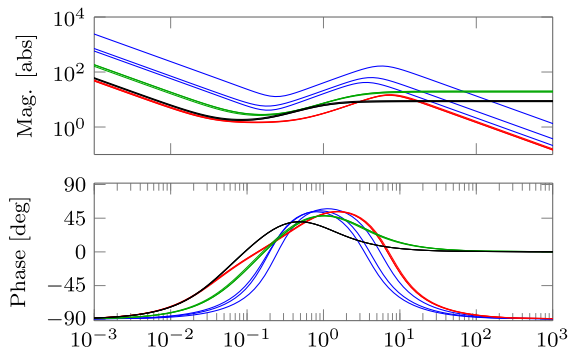


Fig. 7. Bode plot of the obtained controllers for the level control of the lower tank. The different autotuners are ECA (green), Honeywell (black),  $\tau$ -tuner (red) and NOMAD (blue). (For interpretation of the references to color in this figure legend, the reader is referred to the web version of this article.)

that ECA, Honeywell and the  $\tau$ -tuner are very consistent, while NOMAD is varying a bit more due to differences in the estimated models. However, the performance was still similar between the obtained NOMAD controllers.

To evaluate the controller performance two step load disturbances, of equal magnitude but opposite sign, were added to the input of the process. This was done by opening a valve at  $t = 100$  s, decreasing the inflow to the upper tank with 50%, and then closing that valve again at  $t = 300$  s so that all the pumped water once again entered the tank. The performance of the obtained controllers are shown in Fig. 9.

Two versions of the  $\tau$ -tuner are shown in this plot. As was described in Berner et al. (2016b) this autotuner makes some decisions based on the estimated value of the normalized time delay  $\tau$ . In this case the estimated value was low,  $\tau = 0.07$ , and the process was wrongly classified as an integrating model with time delay. The dashed curve shows what the controller performance would have been if the process would instead have been classified as a first-order model with time delay, and the controller tuning would have been based on that. The results indicate that the threshold value for this classification should be reconsidered.

The results show that the NOMAD responds much faster and outperforms the others. The ECA controller comes in second place while

Table 1

PID parameters and IAE values from the level control experiments. For each autotuner three experiments were performed, the chosen parameters for each autotuner are marked with bold text. Note that ECA and Honeywell are on serial form, while  $\tau$ -tuner and NOMAD are on parallel form.

Autotuner	$K$ [-]	$T_i$ [s]	$T_d$ [s]	IAE
ECA	2.06	12.8	3.20	<b>145</b>
	2.24	12.1	3.00	
	<b>2.22</b>	<b>12.2</b>	<b>3.00</b>	
Honeywell	1.52	24.6	6.00	<b>453</b>
	<b>1.41</b>	<b>24.0</b>	<b>6.00</b>	
	1.40	24.0	6.00	
$\tau$ -tuner	1.52	29.7	1.86	<b>518</b>
	1.44	30.7	1.92	
	<b>1.47</b>	<b>30.8</b>	<b>1.92</b>	
NOMAD	4.08	7.07	4.01	<b>51</b>
	12.8	5.33	3.19	
	<b>5.77</b>	<b>8.09</b>	<b>3.66</b>	

the Honeywell controller has too little integral action and recovers very slowly. The  $\tau$ -tuner is about as bad as Honeywell for the solid curve, but improves a bit for the dashed curve.

## 5.2. Temperature control of the batch tank

An illustrative relay experiment for each of the autotuners is shown in Fig. 11. Note that the time scale for this process is in minutes since it is a much slower process than the level control. From the experiment plots it is clear that the Honeywell controller is fastest for this process due to its larger relay amplitudes. The ECA controller is also fast, while the other two are slower. In this case it is not the number of relay switches that influences the experiment duration the most, but rather the time period of the oscillations. Why the different experiments get different time periods is discussed further in Section 6. It is also very clear from the experiment plots that the resolution of the AD-converters is low for this process, the quantization levels are clearly visible.

The controller parameters obtained from the experiments are listed in Table 2, and Bode plots of the controllers are shown in Fig. 10. As can be seen the industrial controllers are both very consistent while the  $\tau$ -tuner and NOMAD are varying more. It can also be noted that the ECA controller chose to use a PI controller for this process, this selection

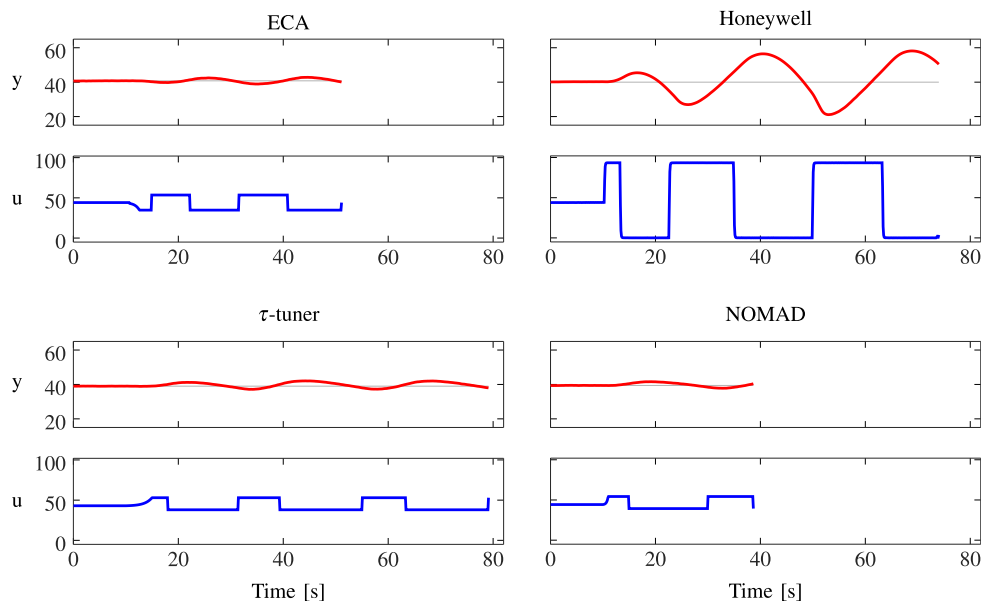


Fig. 8. Relay experiments on the level control of the lower tank for the four autotuners. Note the short experiment time of the NOMAD autotuner and the large control and process deviations of the Honeywell autotuner.

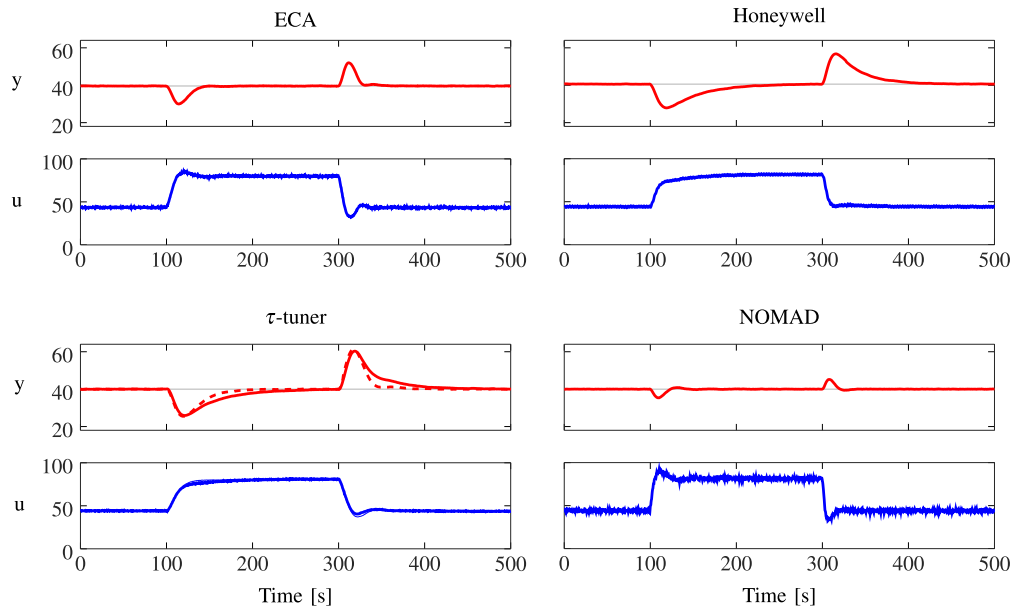


Fig. 9. Controller performance for level control of the lower tank. At  $t = 100$  s a step load disturbance was added to the process input and at  $t = 300$  s that disturbance was removed. The  $\tau$ -tuner has two versions in this plot, one controller based on an integrating model with time delay (solid), and one version tuned from a first-order model with time delay (dashed).

Table 2

PID parameters and IAE values for the temperature control experiments. For each autotuner three experiments were performed, the chosen parameters for each autotuner are marked with bold text. Note that ECA and Honeywell are on serial form, while  $\tau$ -tuner and NOMAD are on parallel form.

Autotuner	$K$ [-]	$T_i$ [s]	$T_d$ [s]	IAE
ECA	10.10	174.7	0	<b>33</b>
	<b>10.36</b>	<b>170.7</b>	<b>0</b>	
	11.12	166.4	0	
Honeywell	33.60	111.6	28.2	<b>15</b>
	<b>33.86</b>	<b>111.6</b>	<b>28.2</b>	
	34.62	109.8	27.6	
$\tau$ -tuner	38.16	88.09	5.51	<b>18</b>
	24.75	46.23	6.94	
	<b>30.16</b>	<b>118.8</b>	<b>7.43</b>	
NOMAD	106.2	39.14	17.2	<b>13</b>
	<b>74.02</b>	<b>45.17</b>	<b>20.0</b>	
	61.39	48.01	20.5	

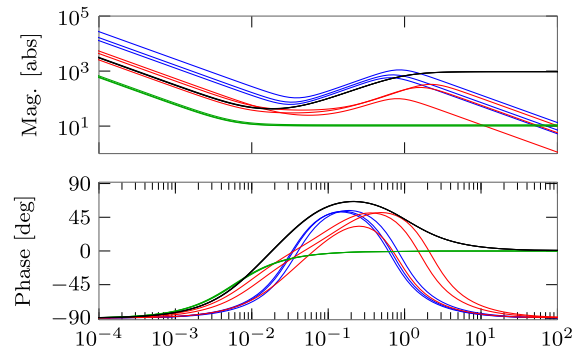


Fig. 10. Bode plot of the obtained controllers for the temperature control of the batch tank. The different autotuners are ECA (green), Honeywell (black),  $\tau$ -tuner (red) and NOMAD (blue). (For interpretation of the references to color in this figure legend, the reader is referred to the web version of this article.)

is a built-in feature of the ECA controller and nothing that we have influenced.

The controller performances for the respective autotuners are shown in Fig. 12. The Honeywell controller performs well on this process, while the ECA is slow and almost not reaching steady-state within the 700 s shown in the plots. The NOMAD and  $\tau$ -tuner performance are quite similar, but the high gain of the NOMAD controller makes it saturate the control signal for a short while in the beginning of the disturbance. They both yield a small overshoot, but recover from it much faster than the ECA does. It can also be noted that even if the Honeywell controller does not have as high gain as the NOMAD and hence rises slightly slower and without an overshoot, the control signal is at least as varying as for the NOMAD controller, due to its large high-frequency gain (seen in Fig. 10) that is amplifying the quantization noise.

### 5.3. Level control of the delayed upper tank

The relay experiments for the delayed tank are shown in Fig. 14. Worth noting in the figure is that both the ECA controller and the  $\tau$ -tuner are adjusting their relay amplitudes during the experiment to decrease the process deviation. This increases the experiment time for them by

a few half-periods. It is also clear from the figure that the Honeywell controller does not perform a good experiment on this process. Its large relay amplitudes make the tank overflow and then become empty at every second relay switch. This makes the result from the Honeywell controller very unreliable for this process, and only one experiment was performed, but the resulting controller parameters will still be used and evaluated for comparison. The obtained controller parameters are listed in Table 3 and Bode plots of the controllers are shown in Fig. 13. From the parameters it is seen that the  $\tau$ -tuner chooses a PI controller since it classifies the process as delay-dominated, see (Berner et al., 2016b) for details on this choice.

The controller performances are shown in Fig. 15. A step load disturbance was introduced at  $t = 100$  s by adding an additional constant flow of water to the tank. The additional flow was removed again at  $t = 800$  s. The NOMAD and  $\tau$ -tuner are showing very good control results for this process, while the ECA is really slow and Honeywell is both oscillating and slow. Comparing the IAE values gives a different message, since the IAE for the Honeywell controller is slightly smaller than for the  $\tau$ -tuner. This implies that IAE should be combined with restrictions on robustness.

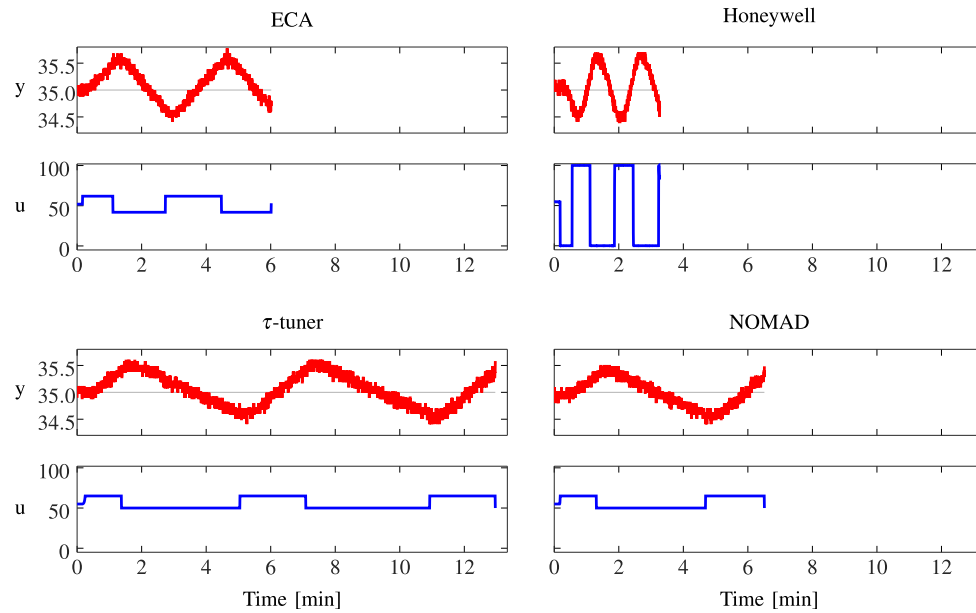


**Fig. 11.** Relay experiments for the temperature control of the batch process. Note that the time scale is in minutes for this process. Also note the different experiment durations that is a consequence of the different oscillation periods, this will be discussed further in Section 6.

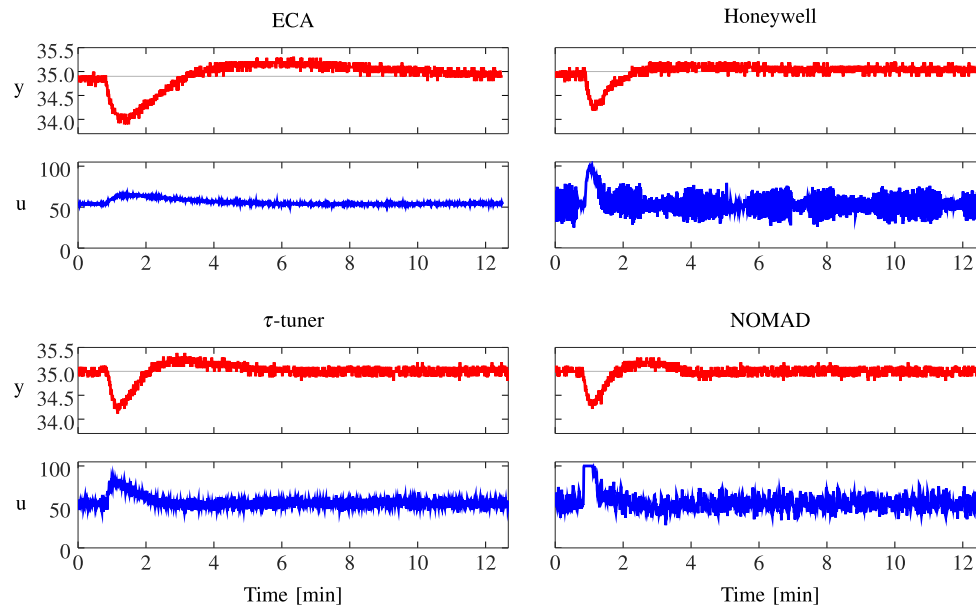


**Fig. 12.** Controller performance for the temperature control of the batch tank. At time 50 s a load disturbance was introduced by changing 20 ml of the heated water to ambient tempered water in the tank.

## 6. Discussion

The results show that ECA is performing well for the level control of the lower tank, but is slow for the other two processes. The autotuner is easy to use, but the user has to ensure that the process is in steady-state before starting the experiment in order to get good results. If the process value is far from the setpoint when starting the experiment, the system will issue a warning, but apart from that it is the user's responsibility to ensure stationarity.

The Accutune III™ in the Honeywell controller works very well for the temperature control process, but yields very slow controllers for the other processes. Its large experiment amplitudes are a problem, especially for the time-delayed process, where they cause the process value to saturate at every switch, resulting in unreliable results and

causing operational problems. The Honeywell controller is branded as a temperature controller so it is not surprising that it gives the best results for the temperature control process. However, since it claims to give good results for any process including those with deadtimes the performance for that process is rather unsatisfactory. The autotuner feature is quite easy to use, and it is not as sensitive to starting in steady-state as the ECA since the experiment is the same no matter if the process value is at the setpoint or not. Since the relay always uses the maximum amplitudes the experiment becomes more or less asymmetric depending on the chosen setpoint. The need to put it in automatic before starting the experiment seems a bit strange since it does not have any appropriate controller parameters for the process yet. However, since the user is supposed to start the tuning procedure right after and it does not have to be steady it does not matter that much.

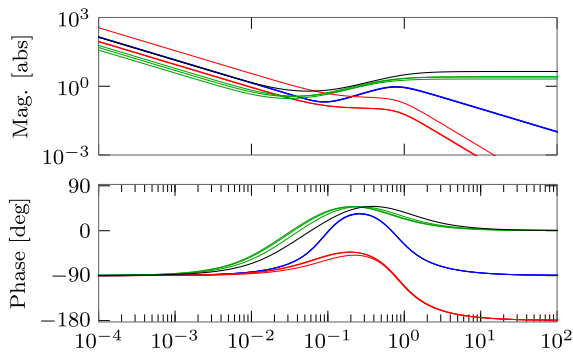


**Fig. 13.** Bode plot of the obtained controllers for the level control of the delayed upper tank. The different autotuners are ECA (green), Honeywell (black),  $\tau$ -tuner (red) and NOMAD (blue). (For interpretation of the references to color in this figure legend, the reader is referred to the web version of this article.)

The  $\tau$ -tuner has an experiment very similar to ECA, except for the asymmetry in the relay. They sometimes differ a few relay switches before convergence is reached, but both the process deviations, amplitude restrictions, and amplitude adjustments are similar. The way of finding models and controller parameters are different though. The results from the  $\tau$ -tuner are slightly worse than ECA for the level control of the lower tank, (especially for the version where the process is classified as integrating), but better than Honeywell. For the temperature control the  $\tau$ -tuner is worse than Honeywell but better than ECA, and for the time-delayed system the  $\tau$ -tuner is much better than both ECA and Honeywell. Overall it can be argued that the  $\tau$ -tuner gives a rather consistent performance. It may not be the best, but it gives acceptable controllers for all the tried processes. The  $\tau$ -tuner, however, suffers the same problem as ECA by requiring the system to be in steady-state before the experiment starts. This is even more crucial for the  $\tau$ -tuner since the asymmetry level of the relay will not be correct if the output is drifting, causing erroneous model estimations. This may be the reason

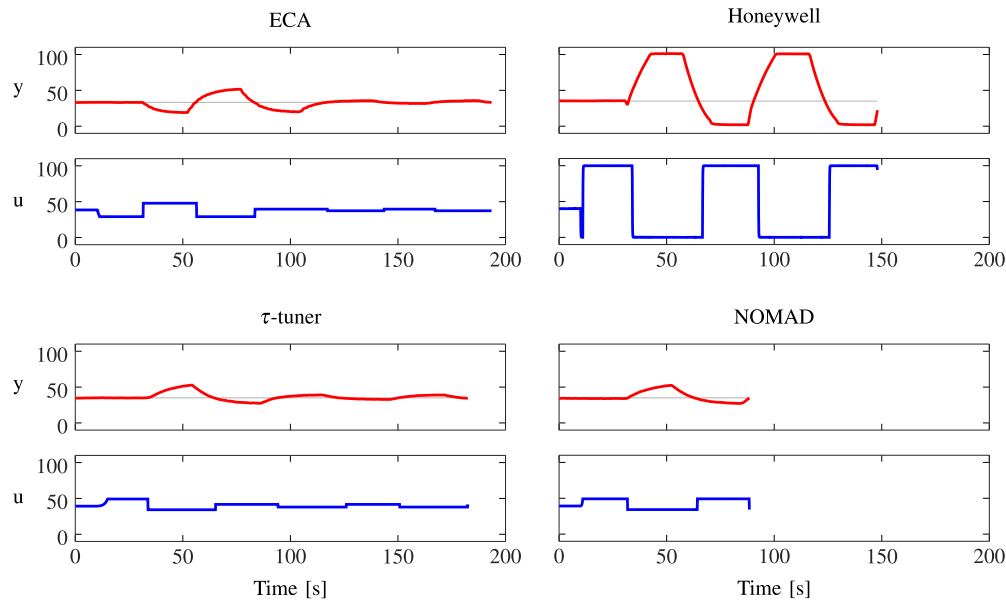


**Fig. 14.** Relay experiments for the level control of the delayed tank. The Honeywell controller is overflowing and emptying the tank at every switch, which make its experiment results unreliable.

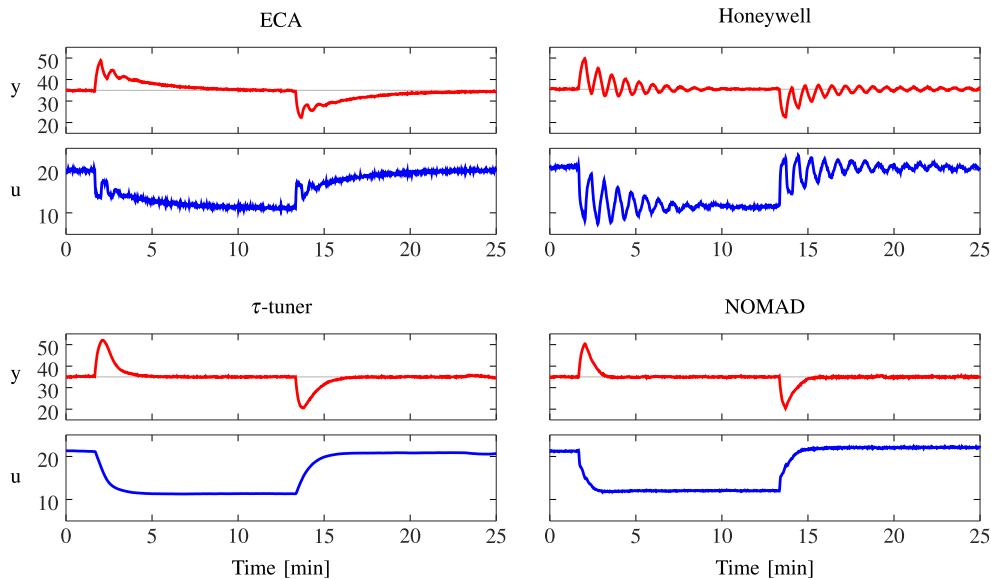


**Fig. 15.** Controller performance for the delayed tank process. A step load disturbance is added to the input at time 100 s and then removed at time 800 s.



**Table 3**

PID parameters and IAE values from the experiments on the upper tank with delay. For most autotuners three experiments were performed, the chosen parameters for each autotuner are marked with bold text. Note that ECA and Honeywell are on serial form, while  $\tau$ -tuner and NOMAD are on parallel form. Since the Honeywell controller was not able to do the experiment without overflowing the tank and emptying it, only one experiment was performed on it.

Autotuner	$K$ [-]	$T_i$ [s]	$T_d$ [s]	IAE
ECA	0.23	61.0	15.2	<b>379</b>
	0.29	48.0	12.0	
	<b>0.28</b>	<b>57.4</b>	<b>14.3</b>	
Honeywell	<b>0.49</b>	<b>36.0</b>	<b>9.00</b>	<b>218</b>
$\tau$ -tuner	0.11	12.3	0	<b>224</b>
	<b>0.11</b>	<b>11.8</b>	<b>0</b>	
	0.32	8.88	0	
NOMAD	0.20	14.7	8.24	<b>152</b>
	0.21	14.6	8.44	
	<b>0.21</b>	<b>14.7</b>	<b>8.32</b>	

why the controller parameters sometimes differ between consecutive experiments for the  $\tau$ -tuner.

The NOMAD autotuner gives best controller performance for all tested processes. The increase in computing to get more accurate models allows for more aggressive controller designs, which is clearly seen for instance in Fig. 9. Even though the response is much faster, the control signals are not much larger than for the other controller designs. Since the NOMAD is using a second-order filter, the noise is not affecting the result much even if the derivative parts of the controller design are large. In fact, looking at the Bode plots it can be seen that both the  $\tau$ -tuner and the NOMAD are less sensitive to high frequency noise than the industrial controllers. Apart from the good performance, the short durations and low process deviations of the experiment are also great benefits of the method. The experiment can also be started with non-stationary initial conditions, so the problem encountered in ECA and the  $\tau$ -tuner to ensure steady state before starting the autotuner is removed. The benefit of short experiment duration is especially useful since it reduces the risk of disturbances entering during the experiment, which is one of the largest risks of failure for the relay autotuners. The experiment is similar to those of both ECA and the  $\tau$ -tuner, but with approximately half the number of relay switches.

As can be seen in Fig. 11, the number of relay switches are not always what is most significant for the experiment duration. If there would have been no hysteresis in the relays, they would all oscillate with the same frequency. With hysteresis the relay amplitudes and hysteresis amplitude will have a large impact on the oscillation period for certain processes. This could be understood by looking at the Nyquist curve in Fig. 16. The approximative describing function method tells that a system under symmetric relay feedback will oscillate with a frequency decided by the intersection of the process' Nyquist curve with the horizontal line with imaginary part

$$\text{Im} = -\frac{\pi h}{4d}, \quad (8)$$

where  $h$  is the hysteresis of the relay and  $d$  is the relay amplitude. The hysteresis levels seem to be quite similar between the different autotuners, but since the relay amplitude is about five times larger for the Honeywell controller than the others it will oscillate with a much higher frequency and shorter period time. The ECA controller has a slightly higher amplitude than the  $\tau$ -tuner and the NOMAD since it allows 10% both up and down, while they have 10% as their large amplitude. Hence ECA gets a faster oscillation than they do. To exemplify, consider the  $\tau$ -tuner. The average relay amplitude is 7.5% and the hysteresis 0.5%. This would give an intersection with imaginary part  $\text{Im} = -0.5\pi/(4 \cdot 7.5) \approx 0.05$ . Looking in Fig. 16 this implies an oscillation period a bit larger than 300 s, which seem to be a reasonable approximation. For processes that do not change so drastically in frequency in this area the difference between oscillation

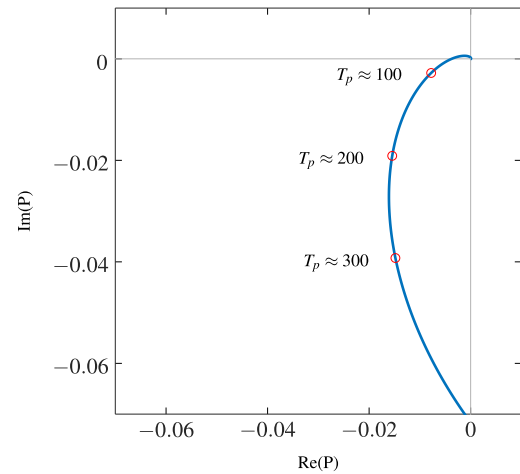


**Fig. 16.** Nyquist plot of the model obtained from the NOMAD autotuner for the temperature control process. Depending on the ratio between relay amplitude and hysteresis, different points on the curve will be intersected by the relay describing function, causing different oscillation periods. Frequencies corresponding to oscillation periods  $T_p = \{100 \text{ s}, 200 \text{ s}, 300 \text{ s}\}$  are marked in the figure.

periods are barely noticeable and for the other experiments in this paper the oscillation periods are therefore more or less the same.

A fundamental benefit of the  $\tau$ -tuner and NOMAD compared to the others is the provision of explicit process models. That makes it possible to change tuning method and filter design without having to perform a new experiment. However, that is mainly a benefit for experienced users or developers. Productized autotuners need to be user-friendly in order to be used. Decisions should be made automatically, maybe allowing, but not requiring, user inputs. Ideally, good results should be provided every time without any manual interaction. The  $\tau$ -tuner and NOMAD-tuner aim for this by making both model and controller selections automatically.

Another feature we propose for the autotuners is that they provide a suitable filter in addition to the controller parameters, since they are strongly connected. ECA does that, and filter designs were included in the implementations of the  $\tau$ -tuner and NOMAD. The autotuner could also propose set-point weighting constants, anti-windup tracking constants and other parameters connected to the PID controller.

## 7. Conclusions and future work

It is time to update the industrial standard autotuners from the 1980's technology to the 21st century. The enormous increase in computing power and data storage provides the possibility to use much more data than just a handful of values from an experiment. By using optimization methods on the entire data set, the experiments can be made shorter and still provide more accurate models, resulting in controllers with better performance. Even though the ECA gives functioning controllers for all processes evaluated in this study, the results show that the NOMAD improves the performance significantly. The NOMAD autotuner also decreases the two main risks of failure for the ECA controller. The first risk is that the process is not in steady-state when the experiment is started. This is handled by the optimization method in NOMAD, that allows non-stationary initial conditions in its estimations. The second main risk is that some disturbance enters the system while the experiment is ongoing, deteriorating the obtained controller. This risk is reduced significantly by the much shorter experiments used in the NOMAD. The short experiments are also very beneficial for the availability of the control loop.

The benefits of the NOMAD autotuner clearly motivates that procedures like it should be productified. The product should have good

and fast implementations of the optimization algorithms, as well as a clear user-friendliness in mind. Because it does not matter how good the autotuner is if it is not used!

## References

- ABB (1999). ECA06/60/600 EMA60 Operator's Manual, ABB Satt AB, doc. number 493-0735-11 (4-1).
- Akaike, H. (1974). A new look at the statistical model identification. *IEEE Transactions on Automatic Control*, 19(6), 716–723.
- Åström, K. J., & Hägglund, T. (1984). Automatic tuning of simple regulators with specifications on phase and amplitude margins. *Automatica*, 20(5), 645–651.
- Åström, K. J., & Hägglund, T. (2006). *Advanced PID control*. Research Triangle Park, NC 27709: ISA - The Instrumentation, Systems, and Automation Society.
- Berner, J., Hägglund, T., & Åström, K. J. (2016a). Asymmetric relay autotuning—Practical features for industrial use. *Control Engineering Practice*, 54, 231–245.
- Berner, J., Hägglund, T., & Åström, K. J. (2016b). Improved relay autotuning using normalized time delay. In *2016 American control conference* (pp. 1869–1875). IEEE.
- Berner, J., & Soltesz, K. (2017). Short and robust experiments in relay autotuners. In *2017 IEEE conference on emerging technologies and factory automation*.
- Chidambaram, M., & Sathe, V. (2014). *Relay autotuning for identification and control*. Cambridge University Press.
- Desborough, L., & Miller, R. (2002). Increasing customer value of industrial control performance monitoring—Honeywell's experience. In *AIChE symposium series* (pp. 169–189).
- Ender, D. B. (1993). Process control performance: Not as good as you think. *Control Engineering*, 40(10), 180–190.
- Friman, M., & Waller, K. V. (1997). A two-channel relay for autotuning. *Industrial and Engineering Chemistry Research*, 36(7), 2662–2671.
- Hast, M., Åström, K., Bernhardsson, B., & Boyd, S. (2013). PID design by convex-concave optimization. In *2013 European control conference* (pp. 4460–4465). IEEE.
- Honeywell (2012). UDC3200 Universal Digital Controller Product Manual, Honeywell, doc. number 51-52-25-119 revision 5.
- Johansson, K. H. (2000). The quadruple-tank process: A multivariable laboratory process with an adjustable zero. *IEEE Transactions on Control Systems Technology*, 8(3), 456–465.
- Kano, M., & Ogawa, M. (2010). The state of the art in chemical process control in Japan: Good practice and questionnaire survey. *Journal of Process Control*, 20(9), 969–982.
- Kaya, I., & Atherton, D. (2001). Parameter estimation from relay autotuning with asymmetric limit cycle data. *Journal of Process Control*, 11(4), 429–439.
- Keyser, R. D., Joita, O. L., & Ionescu, C. M. (2012). The next generation of relay-based PID autotuners (part 2): A simple relay-based PID autotuner with specified modulus margin. *IFAC Proceedings Volumes*, 45(3), 128–133.
- Li, W., Eskinat, E., & Luyben, W. L. (1991). An improved autotune identification method. *Industrial and Engineering Chemistry Research*, 30(7), 1530–1541.
- Liu, T., Wang, Q.-G., & Huang, H.-P. (2013). A tutorial review on process identification from step or relay feedback test. *Journal of Process Control*, 23(10), 1597–1623.
- Luyben, W. L. (1987). Derivation of transfer functions for highly nonlinear distillation columns. *Industrial and Engineering Chemistry Research*, 26(12), 2490–2495.
- Shen, S.-H., Wu, J.-S., & Yu, C.-C. (1996). Use of biased-relay feedback for system identification. *AIChE Journal*, 42(4), 1174–1180.
- Shinskey, F. G. (2002). Process control: As taught vs as practiced. *Industrial and Engineering Chemistry Research*, 41(16), 3745–3750.
- Yu, C.-C. (2006). *Autotuning of PID controllers: A relay feedback approach*. Springer Science & Business Media.